JOURNAL OF MATERIALS SCIENCE **33** (1998) 5119–5124

Breakdown of agglomerates in ideal pastes during extrusion

R. D. WILDMAN
Department of Mechanical Engineering, Loughborough University, Loughborough, Leicestershire L11 3TU, UK
E-mail: r.d.wildman@lboro.ac.uk

S. BLACKBURN
IRC in Materials for High Performance Applications and School of Chemical Engineering, University of Birmingham, Edgbaston, Birmingham B15 2TT, UK

By separating the matrix from the agglomerate it was possible to determine the nature of agglomerate breakdown during extrusion within a known geometry. Previous attempts at observing agglomerate breakdown have been unsuccessful at relating the properties of the paste to the properties of the agglomerate due to the indistinguishability of the paste and the agglomerates. By using well-characterized materials, it was found that the breakdown probabilities of the agglomerates during extrusion were independent of the position of the agglomerate. This indicated that as the shear strain rate was known to be highly position dependent, the agglomerate breakdown was shear strain rate independent. Following breakdown, the distributive mixing was observed to be position dependent.

1. Introduction

Extrusion has been used as a method for the production of ceramics since 1835 when stiff-bodied clays were first made into bricks. The technology changed little until the 1950s when shaping by extrusion became important in a wide range of areas including the food industry, pharmaceuticals, and catalyst support production [1]. A simplified view of an extrudable paste is that it consists of two phases, a liquid and a solid. To achieve a suitably plastic material, a liquid, generally an aqueous solution containing a binder, is added to a solid powder. In the ceramics industry, clay-water suspensions were traditionally used to modify paste rheology, but more recently polymer solutions and gels have been used [2, 3].

Agglomerates can either be naturally occurring or they may be introduced into powders to improve their flow characteristics. They have many serious implications for the ultimate strength and durability of ceramics [4]. If the particle size of a powder is small, say for example less than 100 μm, then the natural adhesion forces are frequently significantly larger than the force of gravity. The adhesion forces become increasingly dominant as the particle size decreases, which leads to serious and potentially detrimental agglomeration. Upon sintering any ceramic precursor, e.g., pastes, compacted powder, or slip cast bodies, the differential shrinkage rates of the agglomerate and the matrix may cause imperfections to occur, producing a significantly weaker material [5].

The deagglomeration of ceramics by extrusion can be seen as an important method of improving the uniformity, and therefore the strength, of the product. It has been noted recently that the process of extrusion is similar to mixing as the paste is subjected to large amounts of shear at the die entry region, which leads to a greater degree of homogeneity in the product than in the pre-extruded mix [6].

Agglomerate breakdown during extrusion has previously been studied in paste systems consisting of commercially available materials [6–8]. Using image analysis, the rate of breakdown was determined for a set of agglomerates that existed in the paste as a result of natural agglomeration processes in fine alumina powders. A problem associated with this technique was that isolation of the dominant factors was difficult to determine. A refinement of this technique was to separate the agglomerates from the matrix. The two separate components were produced and characterized separately, allowing any correlation between the agglomerate properties and the paste rheology to be ascertained once extrusion had been performed.

2. Experimental procedure

2.1. Materials

A system was devised to locate the agglomerates and then determine their behavior during extrusion. Pastes of similar composition, but of differing color, were produced and arranged in such a manner as to enable the insertion of agglomerates into a known plane. Fig. 1 shows the harlequin arrangement employed. This checkered pattern of paste color allowed the plane of insertion to be maintained and also aided in the identification of the approximate location of the agglomerates contained within the extrudate.

TABLE I Proportion of materials used to produce white, black, and red pastes

Ingredient	Proportion, wt%		
	White	Black	Red
Kaolin	76.2	75.7	75.3
PEG 1500	0.2	0.2	0.2
De-ionized water	23.6	23.5	23.3
Carbon black	—	0.6	—
Methyl red (3% solution in ethanol)	—	—	1.2

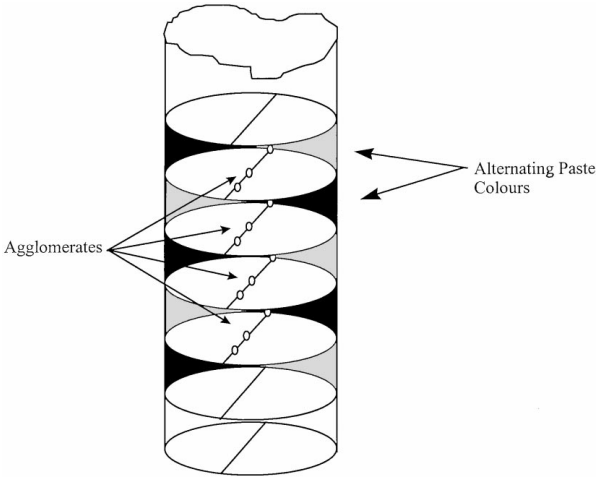

Figure 1 Harlequin arrangement of pastes containing agglomerates.

The pastes consisted of kaolin with polyethylene glycol (PEG 1500) and water acting as a binder, with carbon black and methyl red added as stains. The proportion of each material combined to produce each colored paste is shown in Table I.

2.2. Mixing

The paste was prepared using two mixers to produce a matrix that was mixed well both dispersively and distributively. Initial wetting of the powders was performed using a Kenwood planetary mixer with a whisk attachment. The mixer circulated around the bowl at 66 r.p.m. with the whisk attachment rotating at 140 r.p.m. The geometry of the whisk ensured that all the powder was affected and that compaction was minimized [6]. Pre-mixing continued for two minutes until the powder was completely wetted and a "crumble" was formed. The pre-mixing ensured that the water was distributed about the powder, but the low stresses involved during this process did not allow break-up of fine agglomerates or dispersive mixing to occur. Following pre-mixing and wetting, the "crumble" was transferred to a kneading machine (Werner and Pfleiderer LUK 3 III-2 Vak) that comprised two 125 mm long masticator blades counter-rotating at speeds of 25 and 52 r.p.m. The gap between the blades and the trough wall was measured to be 1.25 mm, resulting in deformation rates of approximately 130 and 270 s^{-1} for the two blades, respectively. To ensure that complete mixing occurred, the walls and blades were scraped free of paste at intervals of 15 min. Following a total mixing time of 45 min, the paste was removed from the kneading machine and placed into an airtight container. The kneading machine forced the paste through repeated large cross-sectional changes by dragging the paste through a narrow gap, creating stresses large enough to break down any visible agglomerates.

2.3. Paste characterization

The rheology of the feed stock material was analyzed using the equations proposed by Benbow and Bridgwater [9] to maintain consistency from batch to batch and also to ensure that the different colored pastes were similar. Extrudable pastes can be considered as two-component systems containing a particulate powder phase and a continuous liquid phase [4]. If a plastic body is forced from a barrel of area A_o into a die of cross-sectional area A_D and length L, then the pressure drop P can be separated into two parts: the pressure required to reduce the cross-sectional area, P_1, and the pressure to push the paste along the die land, P_2. Then, from the theory of plastic extrusion of metals,

$$P_1 = \sigma_y \ln\left(\frac{A_o}{A_D}\right) \tag{1}$$

where σ_y is a uniaxial yield stress [9]. From semi-empirical relationships, the above may be modified by a velocity factor, α, such that

$$P_1 = (\sigma_o + \alpha v) \ln\left(\frac{A_o}{A_D}\right) \tag{2}$$

where v is the velocity of the paste in the die and σ_o is the uniaxial yield stress at zero velocity. The pressure drop P_2 in the die land is opposed by the wall shear stress τ, which, it is argued, is uniform in highly loaded pastes because of plug flow. This can be a velocity-dependent parameter, which by analogy with the uniaxial yield stress can be given by

$$\tau = \tau_o + \beta v \tag{3}$$

where τ_o is the wall shear stress at commencement of movement and β is a factor indicating the change of wall shear stress with velocity. The term βv describes viscous flow in a thin layer at the die wall/paste interface. A force balance gives

$$P_2 = (\tau_o + \beta v) L \left(\frac{E}{A_D}\right) \tag{4}$$

where E is the die perimeter. Thus, the total pressure drop during extrusion is given by

$$\begin{aligned} P &= P_1 + P_2 \\ &= (\sigma_o + \alpha v) \ln\left(\frac{A_o}{A_D}\right) + (\tau_o + \beta v) L \left(\frac{E}{A_D}\right) \end{aligned} \tag{5}$$

For dies and ram extruders of circular cross-section, with diameters D_D and D_o, respectively, this can be simplified to

$$P = 2(\sigma_o + \alpha v)\ln\left(\frac{D_o}{D_D}\right) + (\tau_o + \beta v)4\left(\frac{L}{D_D}\right) \quad (6)$$

Where the binder used in the paste shows non-Newtonian behavior, the velocity can be raised by the powers m and n to provide the required agreement with experimental observations:

$$P = 2(\sigma_o + \alpha_1 v^m)\ln\left(\frac{D_o}{D_D}\right) + (\tau_o + \beta_1 v^n)4\left(\frac{L}{D_D}\right) \quad (7)$$

where α_1 and β_1 (MPa·(m/s)$^{-(n \text{ or } m)}$) are not equal to α and β (MPa·(m/s)$^{-1}$). By using a range of die lengths and ram speeds, it is possible to determine estimates for the values of the paste parameters through graphing or regression techniques [9].

2.4. Agglomerate production

Alumina powder (RA 107LS, Baco U.K.) was used as a source of primary particles for the production of the agglomerates. De-ionized water was used as a binder. To produce agglomerates in the range 1.00–1.18 mm, a pan-granulating machine was employed. The equipment consisted of a 500 mm rotating dish inclined at a 45° angle. A plate was suspended in the dish to deflect the powder as it rotated with the pan, which prevented the majority of the powder from sticking to the dish. A batch size of 500 g of alumina powder was employed, and the pan was rotated at a speed of 33 r.p.m. Moisture was introduced over the whole of the exposed powder surface using an atomized spray. Every 30 s 15 ml of de-ionized water was added, for a total of 6 min. The pan was allowed to continue rotating for 60 s after the final spray to ensure that the moisture was distributed and the system stabilized. The required agglomerates were separated from the bulk of the powder using two sieves, 1.00 mm and 1.18 mm in mesh size. Several batches were mixed together to produce a sufficient number of agglomerates in each size fraction. The moisture content of the agglomerates was tested by measuring the weight loss when placed in an oven at 110 °C overnight.

The strength of the agglomerates were determined by diametrical compaction that consisted of two flat platens that crushed the agglomerates between them. The strength was calculated from

$$\chi_{AGG} = 0.7\left(\frac{4F_o}{\pi d_A^2}\right) \quad (8)$$

where F_o is the load at failure and d_A is the agglomerate diameter [10].

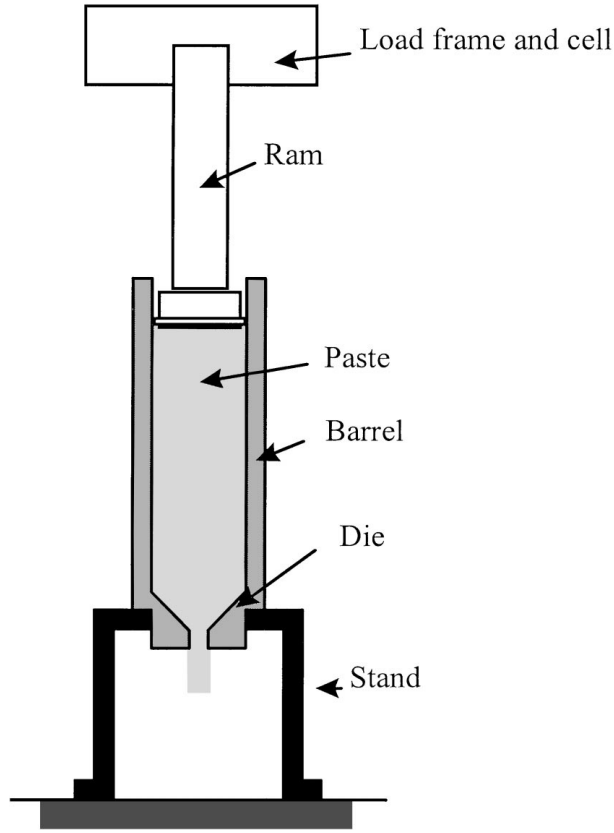

Figure 2 Standard extrusion geometry.

2.5. Extrusion

Discs of paste were produced by first compressing the paste at a pressure of 25 MPa. The paste was then sectioned into discs 10 mm thick and halved. Black and red "half-discs" were pressed together and the agglomerates inserted. The discs were then combined to create a stack. The combination as shown in Fig. 1 was then inserted into the barrel ready for extrusion.

The experimental geometry is shown in Fig. 2. A 45° conical entry die was used to minimize smearing of the extrudate surface. The pastes were extruded at three ram speeds, 10, 50, and 100 mm/min, to enable any variation in agglomerate breakdown with shear strain rate to be observed. A total of 12 agglomerates were subjected to extrusion at each position and ram speed.

2.6. Sample preparation

Following extrusion, the extrudates were sectioned into samples 30–40 mm in length and allowed to dry overnight. The approximate position of a set of agglomerates was determined by observing the relative positions of the colored pastes in the extrudate. The dried extrudates were placed so that the black/red interface, and therefore the agglomerate plane, was parallel to the glass slide and consequently parallel to the plane of grinding. The fixing of the samples was achieved using an epoxy resin adhesive, which was allowed to set over 48 h.

To reduce the possibility of brittle fracture under the forces imposed by grinding, the samples were strengthened by the application of a fast-setting epoxy resin as a

thin supporting layer. This layer was produced by dipping each sample into a bath of epoxy resin after the fixing the extrudates to the glass slide.

2.7. Grinding

The slide holder fixed the extrudate parallel to the grinding wheel. Grinding was completed in set stages at depths of 1.91, 2.29, 2.54, 2.79, and 3.00 mm. The polishing disc, 200 mm in diameter, rotated at a speed of 125 r.p.m. At each stage of grinding, the slide was removed and the extrudate was checked for agglomerates. Any agglomerates that were found could be analyzed, and grinding could then recommence.

2.8. Analysis

When an agglomerate was found, the depth of polishing and the radial position was recorded. The agglomerate was then studied closely using a binocular microscope at a magnification of 50×. Using a scale inserted into one of the objective lenses of the microscope, the dimensions of the agglomerate were determined. The agglomerates were sketched to scale on graph paper to obtain data pertaining to the aspect ratio and the area. Once the agglomerates were sketched, the length and breadth of the agglomerates could be measured using image analysis and the aspect ratio calculated using the relationship

$$\text{Aspect ratio} = \frac{\text{Length}}{\text{Breadth}} \tag{9}$$

Two aspect ratios were measured. First, the total aspect ratio for an associated set of fragments, i.e., the total length divided by the breadth of the widest agglomerate, was measured, and then the length and breadth of each fragment was measured and the average aspect ratio for the associated fragments calculated.

2.9. Fragment size analysis

The data was plotted on a log-normal scale to determine the particle size distribution of the fragments resulting from agglomerate breakdown. Linearity on a scale of this nature indicates that the fragment area distribution followed a log-normal distribution, which can be expressed as follows

$$F(A_{\text{AGG}}) = 1 - \frac{1}{\sqrt{2\pi}K_1} \times \int_{A_{\text{AGG}}}^{\infty} \exp\left(-\frac{1}{2}\left(\frac{\log(A_{\text{AGG}}) - K_{50\%}}{K_1}\right)^2\right) dA_{\text{AGG}} \tag{10}$$

where A_{AGG} is the area fraction, K_1 is the difference in the logarithm of area fraction between 15.87% and 50%, and $K_{50\%}$ is the value of the logarithm of area fraction at the 50% cumulative point [11, 12]. It is known that in dispersions produced by comminution, a log-normal distribution is likely to be seen [13]. The mean area fraction was determined from the 50% cumulative point and then converted to mm^2. The diameter was then calculated from the area fraction.

TABLE II Characterization of pastes using Equation 7

Parameter	White	Black	Red
σ_o (MPa)	0 ± 0	0.16 ± 0.28	0.25 ± 0.22
α_1 (MPa·(m/s)$^{-m}$)	0.89 ± 0.06	2.88 ± 1.96	0.99 ± 1.04
m	0.09 ± 0.02	0.28 ± 0.26	0.66 ± 0.70
τ_o (MPa)	0 ± 0	0 ± 0	0 ± 0
β_1 (MPa·(m/s)$^{-n}$)	0.89 ± 0.05	0.75 ± 0.27	0.77 ± 0.20
n	0.39 ± 0.04	0.28 ± 0.11	0.37 ± 0.06

3. Results

3.1. Paste rheology

Table II shows that the three colored pastes were rheologically similar. The data were a combination of up to five pastes, resulting in the mean and standard deviation given in Table II. This analysis indicates that the yield value associated with parallel flow is zero and that the behavior of the paste, or more specifically the slip layer, corresponds to that seen with a "power law" fluid.

3.2. Agglomerate properties

The moisture content of the agglomerates was measured to be 15.17%, a value associated with moisture present in the atmosphere. The strength of the agglomerates was found to be 0.120 ± 0.013 MPa.

3.3. Total agglomerate aspect ratio

The total agglomerate aspect ratio gives an indication of how much the agglomerate has been stretched out and the degree to which its components have been dispersed. When an agglomerate is extruded, particularly in the system in use here, the majority of the straining forces are experienced at the die entry region. This particular system, consisting of a clay-based paste, has been shown to exhibit plug flow in the barrel and die land region [14]. This implies that in these areas, the agglomerates will only experience the hydrostatic forces due to the increase in pressure required to cause the paste to flow. At the die entry, these forces become hydrodynamic and the shear stress and shear strain rates become non-zero.

Fig. 3 indicates that once break-up occurs, the fragments will tend to be distributed by an amount that depends on the position of the agglomerate. The greatest mixing is observed near the wall, and the amount of distributive mixing is proportional to the distance from the center. The amount of distributive mixing is also seen to be independent of ram speed within the errors associated with the experiment.

3.4. Probability of breakdown

It is sometimes observed that following extrusion, some agglomerates do not suffer breakdown. This is due to

TABLE III Probabilities of breakdown for agglomerates in the size range 1.00–1.18 mm

	Center	Half	Edge
10 mm/min	0.5	0.25	0.57
50 mm/min	0.38	0.4	0.43
100 mm/min	0.57	0.88	0.86
Mean ± Standard Error	0.48 ± 0.06	0.51 ± 0.19	0.62 ± 0.13

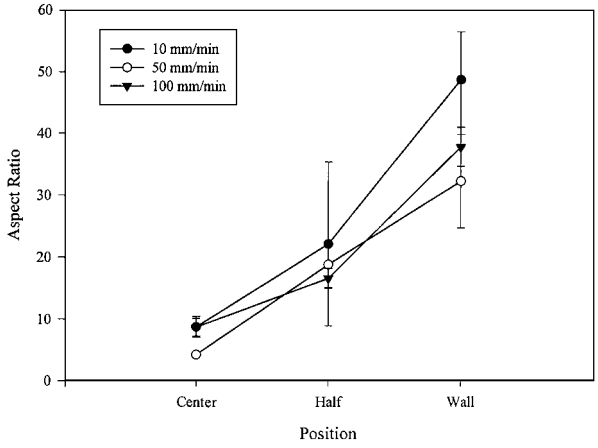

Figure 3 Total agglomerate aspect ratio of fragmented agglomerates following extrusion at a ram speed of 10 mm/min.

the distribution of agglomerate strengths. Therefore, the probability that an agglomerate, from a set of agglomerates of known mean strength, will break down will increase as the stress during extrusion is increased.

One measure of the probability of an agglomerate breaking down is simply the fraction of agglomerates that have been observed to suffer breakdown,

$$\Pr(\text{Breakdown}) = \frac{\text{Number of agglomerates broken up}}{\text{Number of agglomerates found}} \quad (15)$$

This probability then gives an indication of the relative forces likely to be experienced by an agglomerate.

Table III shows the calculated probabilities of breakdown. They indicate no clear correlation between breakdown probability and ram speed. The data indicates that within experimental errors there are only small changes in breakdown probability with position and that these can be neglected.

3.5. Average individual aspect ratio

Fig. 4 shows the average individual aspect ratios for all the ram speeds and initial sizes of agglomerate. This is the average aspect ratios of the fragments as opposed to a measure of the distributive mixing of the fragments. The data show that there is little difference in behavior of the agglomerates regardless of the speed of extrusion, which has already been seen to have a negligible influence on the agglomerate breakdown, and these results confirm these earlier conclusions [6, 14]. The fragments

TABLE IV Average maximum aspect ratios

	Center	Half	Edge
Average Maximum Aspect Ratio	3.467 ± 0.369	3.299 ± 0.174	4.468 ± 0.435

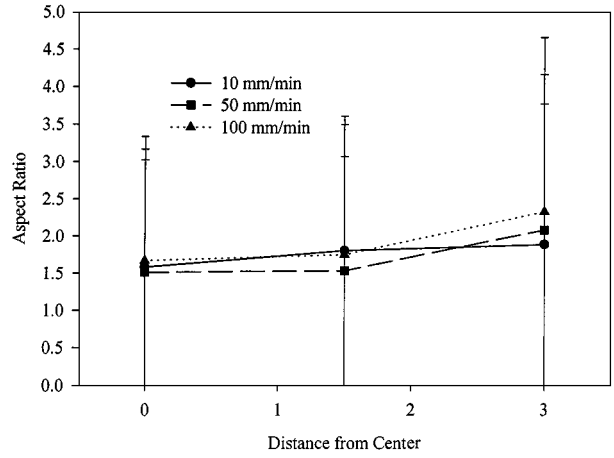

Figure 4 Average individual fragment aspect ratios for extrusion performed at ram speeds of 10, 50, and 100 mm/min.

situated at the edge are seen to have a slightly higher aspect ratio than those situated at other points. This implies that those agglomerates at the edge have either suffered a greater strain before fracture has occurred or they have been exposed to a straining force for a longer time, resulting in the greater strain.

3.6. Maximum aspect ratios

The maximum aspect ratio from each set of agglomerates at three speeds was taken, and the average maximum aspect ratio for each position was calculated. Table IV shows that the largest maximum aspect ratio is observed at the edge positions. The maximum aspect ratios observed at the half and center positions are similar, and quite clearly lower than that observed at the edge. This is similar to that observed in Fig. 4, where the edge aspect ratio is larger than that seen at the center and half positions. This implies again that either the level of stress or the time of straining is different at the edge compared to a position within the body of the paste.

3.7. Fragment size distribution

The diameters associated with the average area fraction of the agglomerates were calculated with the aid of Fig. 5 and are shown in Table V, which shows that the mean size of the fragments were independent of the speed of extrusion. The mean sizes of the fragments were in the range 200–300 μm, whereas the primary particle size of the alumina powder was 1 μm. This indicated that there were several levels of bonding involved in the formation of agglomerates and that either the dispersion forces involved in extrusion were only strong enough to break down the agglomerates partially

TABLE V Mean size and standard deviation of agglomerate fracture products following extrusion

Initial Agglomerate Size	10 mm/min	50 mm/min	100 mm/min
1.00–1.18 mm	0.24 ± 0.04 mm	0.27 ± 0.04 mm	0.24 ± 0.03 mm

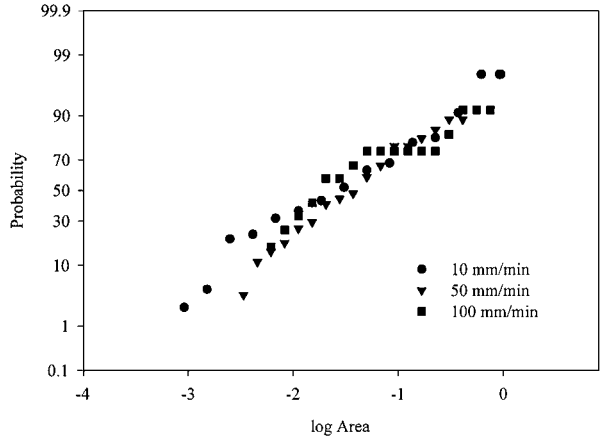

Figure 5 Log-normal probability graph of the fracture fragments of agglomerates following extrusion.

or that the agglomerates did not spend sufficient time subjected to the required forces.

4. Discussion

The breakdown probability of the agglomerates can be related to the stress to which they are subjected. Within a batch of agglomerates, there is a distribution of the agglomerate strengths. Therefore, when a batch of agglomerates is subjected to a fixed stress, a proportion will be seen to fail, depending on the level of the stress compared to the strength distribution of the agglomerate. A higher stress will result in a higher proportion of agglomerates being broken down. Therefore, as the proportion of agglomerates suffering breakdown is similar regardless of position, it can be assumed that the break-up stress is independent of the position of the agglomerate, i.e., the fluid is imparting a constant stress across the radius of the barrel/die arrangement. Once fragmentation has occurred, the behavior of the agglomerate is then highly dependent on position. The fragments at the wall are distributed up to 6 times as much as those at the center. Following the break-up of the agglomerates, the strain behavior of the materials is the dominant factor.

5. Conclusions

It has been found that the distributive mixing action of extrusion varies as a function of position across the barrel or die. The probability of break-up of the agglomerates is a good indication of the power of the dispersion forces involved during extrusion. There was no clear trend across the barrel, neither increasing nor decreasing, that clearly indicated significant differences in dispersion with position. This indicated that in extrusion, distributive mixing is position dependent, whereas dispersion is geometry dependent. The fragment size distribution followed a log-normal distribution, commonly seen in comminution studies. Analysis of the mean sizes also indicated that the break-up forces were independent of the ram speed.

Acknowledgements

The authors would like to acknowledge the support of the EPSRC and the National Physical Laboratory (under a Department of Trade and Industry–funded project on Materials Metrology).

References

1. A. T. GREEN and G. H. STEWART, in "Ceramics" (British Ceramics Society, Stoke-on-Trent, 1953).
2. K. JIRATORA, L. JANACEK and P. SCHNEIDER, in "Studies in Surface Science and Catalysis 16, Preparation of Catalysts III", edited by G. Pancelet, P. Grange and P. A. Jacobs (Elsevier, Amsterdam, 1983).
3. J. F. WHITE and A. L. CLAVEL, *Am. Ceram. Soc. Bull.* **42** (1968) 698.
4. F. F. LANGE, *J. Am. Ceram. Soc.* **67** (1984) 83.
5. K. KENDALL, *Powder Met.* **31** (1988) 28.
6. H. BÖHM and S. BLACKBURN, *Brit. Ceram. Trans.* **93** (1994) 169.
7. Idem., *IChemE Research Event* (1993) 705.
8. R. D. WILDMAN and S. BLACKBURN, *ibid.* (1995) 838.
9. J. J. BENBOW and J. BRIDGWATER, in "Paste Flow and Extrusion" (Oxford University Press, Oxford, 1993).
10. Y. HIRAMATSU and Y. OKA, *Int. J. Rock. Min. Sci.* **3** (1966) 89.
11. W. C. HINDS, in "Aerosol Technology" (Wiley Interscience, New York, 1982).
12. S. P. RWEI and I. MANAN-ZLOCZOWER, *Polymer Engng. Sci.* **30** (1990) 701.
13. P. C. HIEMENZ, in "Principles of Colloid and Surface Chemistry" (Marcel Dekker Inc., New York, 1986).
14. R. D. WILDMAN, Ph.D. thesis, University of Birmingham, Birmingham UK, (1997).

Received 23 July
and accepted 17 August 1998